

## Open heavy flavor production from light ion collisions at RHIC

Y. Kwon<sup>1</sup> for the PHENIX collaboration

<sup>1</sup>Dept. of Physics, Univ. of Tennessee, Knoxville, TN 37996, USA

**Abstract.** PHENIX measures leptons at mid and forward rapidities and extracts leptons resulting from semi-leptonic decays of heavy quarks. We present PHENIX results related to heavy quark production, specifically the invariant cross section of the non-photonic single electrons produced at midrapidity in  $p+p$  and  $d+Au$  collisions at  $\sqrt{s_{NN}} = 200$  GeV. The measured cross section for  $p+p$  collisions is compared with the NLO prediction, and a possible excess over the prediction is noted. The measured cross section for  $d+Au$  collisions scales with the number of colliding nucleon pairs from the  $p+p$  spectra.

*Keywords:* Non-photonic single electron, heavy quark, pQCD  
*PACS:* 25.75.Dw

### 1. Introduction

The parton model and perturbative Quantum Chromodynamics (pQCD) can be applied to the violent strong interaction processes characterized by a large scale [ 1]. As an example, it is applied to the hard particle production where  $p_T$  serves as the large scale. Neutral pion production in  $p+p$  collisions at  $\sqrt{s} = 200$  GeV in the range  $2 < p_T < 13$  GeV/c measured by the PHENIX experiment at RHIC can be well described by the Next-to-Leading-Order (NLO) pQCD [ 2].

Heavy quark production belongs to the category of violent strong interaction processes due to its large mass. While classification of the charm quark as a heavy quark is not yet fully settled [ 1], the parton model and pQCD are often applied to the charm quark production. Within the given limitations, predictions for charm hadro-production exist from lower collision energies including the Fermi Lab fixed target program [ 3].

Further predictions were made for heavy quark production in the ion collisions. Systematic studies of charm production in  $p+p$  and  $p+$ nucleus collisions have been proposed as a sensitive way to measure the parton distribution function in nucleons,

and nuclear shadowing effects [ 4]. For heavy ion collisions at RHIC energies, heavy quark energy loss [ 5], modification of charm quark hadronization [ 6], in-medium effects on open- and hidden-charm states [ 7], possible  $J/\psi$  suppression [ 8], and charm flow [ 9] have been proposed as possibilities.

## 2. Theoretical background

Factorization of the hadro-production cross section of heavy flavored hadrons is described as follows. The differential cross-section for the production of a heavy flavored particle (a charmed particle in the particular case),  $H$ , in the collision of two hadrons,  $A$  and  $B$ , is believed to factorize in the following manner [ 1],

$$d\sigma[A+B \rightarrow H+X] = \sum_{ij} f_{i/A} \otimes f_{j/B} \otimes d\hat{\sigma}[ij \rightarrow h\bar{h}+X] \otimes D_{h \rightarrow H} + remainder \quad (1)$$

Here  $i,j$  denote partons which are point-like,  $f_{i/A}$  and  $f_{j/B}$  are parton distribution functions, and  $D_{h \rightarrow H}$  is the fragmentation function for the heavy quark  $h$  hadronizing into  $H$ . The parton distribution functions and the fragmentation functions are process independent. The  $d\hat{\sigma}[ij \rightarrow h\bar{h}+X]$  is a perturbatively calculable short-distance cross section. The remainder represents corrections to the factorized form of the cross section that are power-suppressed by  $\Lambda_{QCD}/m_h$  or possibly  $\Lambda_{QCD}/p_T$  if  $p_T \gg m_h$ . A large quark mass  $m_h$  makes the remainder smaller, and application of pQCD to the factorized term becomes possible.

As the collision energy increases, the factorized term increases faster than the remainder, and the hard processes (factorized term) gain importance at high collision energies. We can test the validity of the factorization at RHIC collision energies by measuring heavy flavored hadron production for  $p+p$  collisions.

The factorization scheme has further consequences for the collisions of ions. For the interaction between point-like partons, we can approximate the nuclear parton distribution as follows.

$$f_{i/Au} \approx 79 f_{i/p} + 118 f_{i/n} \approx 197 f_{i/N},$$

and

$$f_{i/d} \approx f_{i/p} + f_{i/n} \approx 2 f_{i/N}$$

where  $f_{i/N}$  is the parton distribution function inside the nucleon.

If the charm producing processes are point-like and there is no modification of the initial parton distribution for the  $d + Au$  collisions, the charm production cross section will scale with  $2 \times 197$ , i.e. the number of colliding nucleon pairs. Surprisingly, this extension does not work for high  $p_T$  particles produced in central Au+Au collisions [ 12], and careful studies of the stated scaling are desirable for the various hard processes.

### 3. Measurements

PHENIX is capable of measuring leptons at mid and forward rapidities. PHENIX uses global detectors to characterize the collisions, a pair of central spectrometers at mid rapidity to measure electrons, hadrons, and photons, and a pair of forward spectrometers to measure muons. Each spectrometer has a large geometric acceptance of about one steradian, excellent energy and momentum resolution, and particle identification (see Fig. 1).

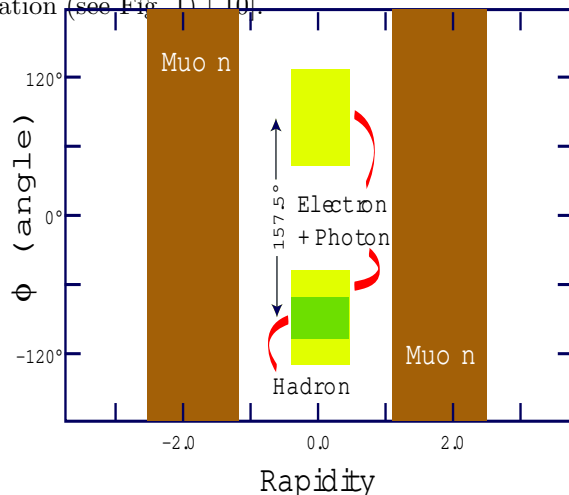


**Fig. 1.** Acceptance of the PHENIX experiment.

The PHENIX central arms consists of tracking systems for charged particles and electromagnetic calorimetry. The calorimeter is the outermost subsystem of the central arms and provides measurements of both photons and energetic electrons. The tracking system uses three sets of Pad Chambers (PC) to provide precise three-dimensional space points needed for pattern recognition. The precise projective tracking of the Drift Chamber (DC) is the basis of the excellent momentum resolution. A Time Expansion Chamber (TEC) in the east arm provides additional tracking and particle identification. The Time-of-Flight (ToF) and Ring-Imaging CHerenkov (RICH) detectors provide particle identification. The RICH provides separation of electrons from the large number of copiously produced pions. Using information from the RICH, the TEC, and the electromagnetic calorimeter it is possible to reject pion contamination of identified electrons to one part in  $10^4$  over a wide range of momenta.

Each forward spectrometer is based on a muon tracker inside a radial magnetic field followed by a muon identifier, both with full azimuthal acceptance. The muon trackers consist of three stations of multiplane drift chambers that provide precision tracking. The muon identifier consist of alternating layers of steel absorbers and low resolution tracking layers of streamer tubes of the Iarocci type. With this combination, the pion contamination of identified muons is typically  $3 \times 10^{-3}$ , and can

be estimated and subtracted statistically. Measurement of *prompt muons* resulting from semi-leptonic decays of heavy flavored hadrons is also possible, and analysis is actively pursued.

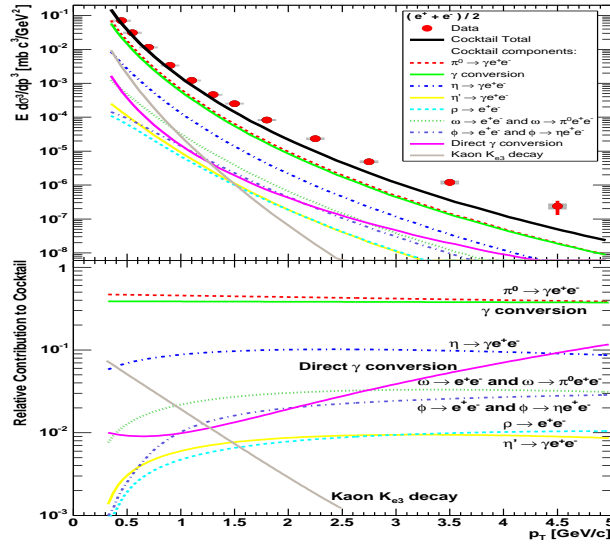


**Fig. 2.** The inclusive single electron spectra and composition of backgrounds,  $p+p$  collisions at  $\sqrt{s_{NN}} = 200$  GeV.

PHENIX measures the non-photonic single electron spectra by first measuring the inclusive electron spectra and then subtracting the contribution from photonic sources. Inclusive electrons contain two components: (1) *non-photonic* - primarily semi-leptonic decays of mesons containing heavy (charm and bottom) quarks, and (2) *photonic* - Dalitz decays of light neutral mesons ( $\pi^0$ ,  $\eta$ ,  $\eta'$ ,  $\rho$ ,  $\omega$ , and  $\phi$ ) and photon conversions in the detector material. The PHENIX experiment uses two approaches, *converter subtraction* and *cocktail subtraction*, to estimate the photonic component.

The converter subtraction is a data-driven approach. A photon converter (a thin brass tube of 1.7% radiation length thick) is installed in the middle of data-

taking. The photon converter multiplies the photonic contribution to the electron yield in a well-defined manner and hence the photonic component can be estimated.

The cocktail subtraction simulates electron production from the known sources and subtract them from the inclusive spectra. PHENIX has measured the  $p_T$  distributions of  $\pi^\pm$  and  $\pi^0$ . We fit a power law function to the combined data sets to determine the input  $\pi^0$  spectrum for the decay generator. The  $p_T$  distribution of any other hadrons is obtained from the  $\pi^0$  spectrum by replacing  $p_T$  with  $\sqrt{p_T^2 + m_h^2 - m_{\pi^0}^2}$ . In this parameterization  $h/\pi^0$  ratios approach constants at high  $p_T$ . The asymptotic ratios used to fix the relative normalizations are determined from the world data including the PHENIX results. Photon conversions are evaluated using a combination of the GEANT simulation and the hadron decay generator.

The converter subtraction and the cocktail subtraction yield consistent results, and Fig. 2 shows the inclusive electron spectra and composition of the estimated background.

## 4. Result

The cocktail subtracted invariant electron cross section is shown on Fig. 3. The PYTHIA calculation ( $m_c = 1.25 \text{ GeV}/c^2$ ,  $m_b = 4.1 \text{ GeV}/c^2$ ,  $K = 3.5$ , and  $< k_t > = 1.5$ ) is displayed on the same figure. The NLO pQCD prediction of heavy flavor-related electrons was made using the HVQLIB package. The heavy quark production cross section was calculated using HVQLIB and PYTHIA, and the ratio of heavy quark yields  $(dN_q/dp_T)_{HVQLIB}$  to  $(dN_q/dp_T)_{PYTHIA}$  was used as a weight for the PYTHIA decay electrons. This method enables us to use an exact NLO pair production calculation together with fragmentation and decay kinematics from PYTHIA. Within the NLO pQCD calculation, charm decays are the major source of non-photonic single electrons for most of the observed  $p_T$  range. The NLO prediction for open charm yields harder spectra than the PYTHIA calculation, but an excess of data over both predictions is seen beyond intermediate  $p_T$ . An elaborate theoretical study has appeared recently and also shows the observed excess [ 11]. The uncertainty of theoretical prediction mostly comes from the mass and the scale uncertainties, and is relatively large. Reduced experimental errors will contribute to a definitive statement.

Fig. 4 shows both the non-photonic single electron production in the  $d+Au$  collisions at  $\sqrt{s_{NN}} = 200 \text{ GeV}$  scaled with the number of colliding nucleon pairs, described in section 2, and the empirical parametrization of  $p+p$  production. We observe that the non-photonic single electron production in the  $d+Au$  collisions scales with the number of colliding nucleon pairs. Further study was made for four centrality classes. Non-photonic single electron spectra obtained from each centrality class are also consistent with the  $p+p$  spectra scaled by the nuclear thickness. The observation is consistent with the picture of non-photonic single electrons produced by point-like interactions.

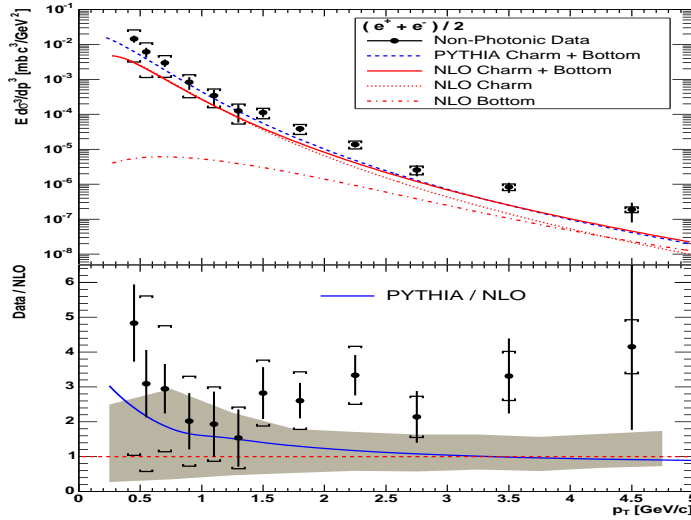


**Fig. 3.** The non-photonic single electron spectra from the  $p+p$  collisions at  $\sqrt{s_{NN}} = 200 \text{ GeV}$  and comparison with the NLO pQCD prediction.

## 5. Conclusion

We have discussed exciting theoretical and experimental aspects of heavy quark production with emphasis on quantities measurable by PHENIX. Selected results from PHENIX were presented and we note key experimental observations.

a) The non-photonic single electron spectra from  $p+p$  collisions at  $\sqrt{s_{NN}} = 200 \text{ GeV}$  indicate a possible excess over the NLO pQCD heavy quark prediction.

b) Within errors, the non-photonic single electron spectra obtained from  $d+Au$  collisions both in minimum bias or in various centrality classes exhibits scaling with the number of colliding nucleon pairs from the  $p+p$  spectra. Hence, production process for non-photonic single electrons is consistent with point-like interactions.

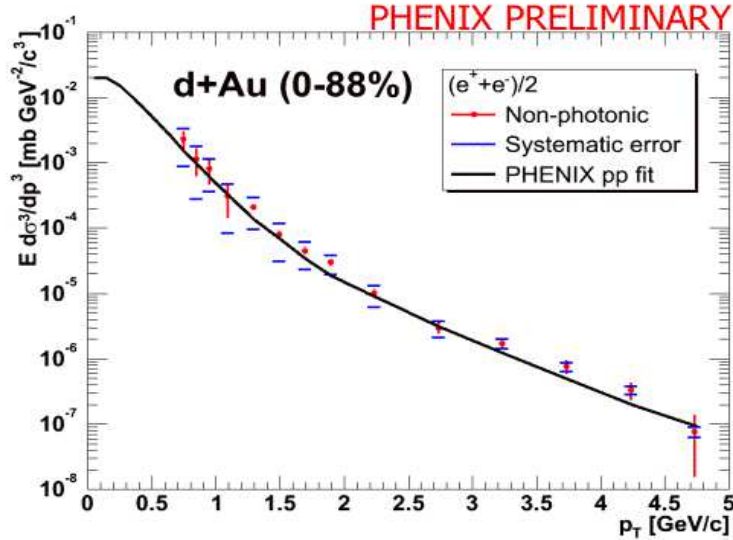


**Fig. 4.** The non-photonic single electron spectra from the  $d+Au$  collisions at  $\sqrt{s_{NN}} = 200 \text{ GeV}$  (scaled with the number of colliding nucleon pairs). The empirical parametrization of the  $p+p$  spectra is also displayed.

## Acknowledgment

We thank the staff of the Collider-Accelerator and Physics Departments at BNL for their vital contributions. We acknowledge supports from the Department of Energy and NSF (U.S.A.), MEXT and JSPS(Japan), CNPq and FAPESP(Brazil), NSFC(china), CNRS-IN2P3 and CEA(France), BMBF, DAAD, and AvH (Germany), OTKA(Hungary), DAE and DST(India), ISF(Israel), KRF and CHEP(Korea), RMIST, RAS, and RMAE (Russia ), VR and KAW (Sweden), U.S. CRDF for the FSU, US-Hungarian NSF-OTKA-MTA, and US-Israel BSF.

## References

1. J. C. Collins, D. E. Soper and G. Sterman, Nucl. Phys. B **263**, 37 (1986).
2. S. S. Adler et al. (PHENIX), Phys. Rev. Lett. **91**, 241803 (2003).
3. M. L. Mangano et al., Nucl. Phys. B **405**, 507 (1993).
4. Z. Lin and M. Gyulassy, Phys. Rev. Lett. **77**, 1222 (1996).
5. Y. L. Dokshitzer and D. E. Kharzeev, Phys. Lett. B **519**, 199 (2001).
6. A. Andronic et al., Phys. Lett. B **571**, 36 (2003), R. L. Thews, M. Schroedter, and J. Rafelski, Phys. Rev. C **63**, 054905 (2001).

- 
7. L. Grandchamp, R. Rapp, G. E. Brown, Phys. Rev. Lett. **92**, 212301 (2004).
  8. T. Matsui and H. Satz, Phys. Lett. B **178**, 416(1986).
  9. V. Greco, C. M. Ko and R. Rapp, Phys. Lett. B **595**, 202(2004).
  10. K. Adcox et al. (PHENIX), NIM A **499** 469 (2003).
  11. M. Cacciari, P. Nason, R. Vogt, <http://arxiv.org/abs/hep-ph/0502203>.
  12. S. S. Adler et al., Phys. Rev. Lett. **91**, 072303 (2003).